

Synthesis and Reactivities of Guanidinate Dianion Complexes of Heterobimetallic Lanthanide–Lithium $\text{Cp}_2\text{Ln}[(\text{CyN})_2\text{CNPh}]\text{Li}(\text{THF})_3$

Pengzhi Zheng,[†] Jianquan Hong,[†] Ruiting Liu,[†] Zhengxing Zhang,[†] Zhen Pang,[†]
Linhong Weng,[†] and Xigeng Zhou^{*,†,‡}

[†]Department of Chemistry, Shanghai Key Laboratory of Molecular Catalysis and Innovative Materials, Fudan University, Shanghai 200433, People's Republic of China, and [‡]State Key Laboratory of Organometallic Chemistry, Shanghai 200032, People's Republic of China

Received December 11, 2009

The treatment of Cp_3Ln with 1 equiv of N,N' -dicyclohexyl- N'' -phenylguanidine followed by reacting with butyllithium yields a series of novel guanidinate dianion complexes of heterobimetallic lanthanide–lithium with formula $\text{Cp}_2\text{Ln}[(\text{CyN})_2\text{CNPh}]\text{Li}(\text{THF})_3$ ($\text{Ln} = \text{Yb}$ (**1a**), Er (**1b**), Y (**1c**), Dy (**1d**)). Reactivities of these dianionic guanidinate complexes toward various electrophiles have been investigated. Reaction of **1** with Me_2RSiCl produced tetrasubstituted guanidinate monoanion complexes $\text{Cp}_2\text{Ln}[(\text{CyN})_2\text{CN}(\text{Ph})\text{SiRMe}_2]$ ($(\text{R} = \text{Me}, \text{Ln} = \text{Yb}$ (**2a**), Er (**2b**), Y (**2c**); $\text{R} = \textit{i}$ Bu, $\text{Ln} = \text{Yb}$ (**3a**), Er (**3b**)), indicating that the Li–N bond is preferred to couple with chlorosilanes. In contrast, the regioselective functionalization of the NCy group bonded to the lanthanide ion was achieved by reaction of **1a** with Me_2SiCl_2 to produce $\text{Me}_2\text{Si}(\text{CyN})_2\text{C}=\text{NPh}$ (**4**) and $\text{Cp}_2\text{YbCl}(\text{THF})$ (**5**). Significantly, treatment of **1d** with PhCOCl leads to the cleavage of one C–N bond of the dianionic guanidinate, giving the acylamino complex $[\text{Cp}_2\text{Dy}(\text{OC}(\text{Ph})\text{NCy})_2]$ (**6**). These results have shown that the active site of the dianionic guanidinate ligand is tunable due to the delocalization of the two negative charges on the three N atoms. All the compounds were characterized by elemental analysis and spectroscopic methods. The structures of compounds **1–6** are also determined through X-ray single-crystal diffraction analysis.

Introduction

Considerable recent interest has focused on the development of guanidinate anions as sterically and electronically flexible ligands for the design of new metal complexes. Among them guanidinate monoanions are well established as versatile ligands for a remarkably wide range of metals. A major impetus for such studies can be traced to the well-known applications of guanidinate metal complexes in homogeneous catalysis¹ and materials science.² In contrast, the guanidinate dianion complexes have received very limited attention as ligands in organometallic and coordination chemistry. This is surprising, given the expectation that the guanidinate dianion ligands should lead to novel coordination properties and may impart an enhanced reactivity to the corresponding metal complexes due to the presence of an added anionic nitrogen center and thus generating a unique, conjugated π system. For example, transition-metal guanidinate dianion complexes have been implicated as reaction intermediates in glynylation of amines with carbodiimides³

and transamination,⁴ which highlight the value of such species. There does not appear to be a large effort to expand upon this class of compounds, which is probably due to the lack of convenient synthetic methodologies to access these complexes. Dianionic guanidinate complexes are rare and are mainly prepared by the cycloaddition of transition-metal imido complexes with carbodiimides.^{4,5} Only a few dianionic guanidinate ligands are introduced by deprotonation of monoanionic guanidates using alkyl⁶ or amido⁷ metal reagents. Therefore, it is highly desirable to develop new dianionic guanidinate complexes and a new method for their construction.

On the other hand, there is currently considerable interest in studying the reactivities of the Ln–N bond of lanthanide amides due to their applications in organic synthesis and catalysis.⁸ Nonetheless, research efforts are primarily

*Corresponding author. E-mail: xgzhou@fudan.edu.cn.

(1) (a) Edelmann, F. T. *Chem. Soc. Rev.* **2009**, *38*, 2253. (b) Edelmann, F. T. *Adv. Organomet. Chem.* **2008**, *57*, 183.

(2) (a) Milanov, A. P.; Fischer, R. A.; Devi, A. *Inorg. Chem.* **2008**, *47*, 11405. (b) Milanov, A.; Bhakta, R.; Baunemann, A.; Becker, H. W.; Thomas, R.; Ehrhart, P.; Winter, M.; Devi, A. *Inorg. Chem.* **2006**, *45*, 11008.

(3) Blake, A. J.; McInnes, J. M.; Mountford, P.; Nikonov, G. I.; Swallow, D.; Watkin, D. J. *J. Chem. Soc., Dalton Trans.* **1999**, 379.

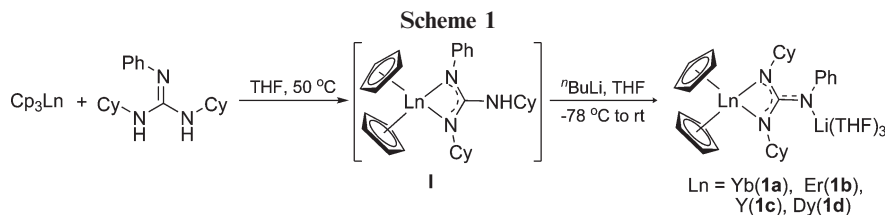
(4) Ong, T. G.; Yap, G. P. A.; Richeson, D. S. *Chem. Commun.* **2003**, 2612.

(5) (a) Ong, T. G.; Yap, G. P. A.; Richeson, D. S. *J. Am. Chem. Soc.* **2003**, *125*, 8100. (b) Zuckerman, R. L.; Bergman, R. G. *Organometallics* **2001**, *20*, 1792. (c) Zuckerman, R. L.; Bergman, R. G. *Organometallics* **2000**, *19*, 4795. (d) Birdwhistell, K. R.; Lanza, J.; Pasos, J. J. *Organomet. Chem.* **1999**, *584*, 200.

(6) Chivers, T.; Parvez, M.; Schatte, G. *J. Organomet. Chem.* **1998**, *550*, 213.

(7) (a) Tin, M. K. T.; Thirupathi, N.; Yap, G. P. A.; Richeson, D. S. *J. Chem. Soc., Dalton Trans.* **1999**, 2947. (b) Tin, M. K. T.; Yap, G. P. A.; Richeson, D. S. *Inorg. Chem.* **1999**, *38*, 998. (c) Bailey, P. J.; Gould, R. O.; Harmer, C. N.; Pace, S.; Steiner, A.; Wright, D. S. *Chem. Commun.* **1997**, 1161.

(8) Hong, S.; Marks, T. J. *Acc. Chem. Res.* **2004**, *37*, 673.



focused on monoanionic amido lanthanide complexes.⁹ To our knowledge, the selective reaction involving the dianionic guanidinate ligands in organolanthanide chemistry has remained unexplored to date, probably due to the lack of suitable complexes. The scarcity of lanthanide complexes supported with dianionic nitrogen-centered ligands warrants exploration of guanidinate dianion ligands in this regard. Recently, we have reported the synthesis of the first guanidinate dianion complexes of rare earth metals, which are formed by the unexpected disproportionation of monoanionic pyridyl-substituted guanidinate ligands.¹⁰ To elucidate the structure–reactivity relationship of lanthanide guanidinate dianion complexes, we are interested in developing new targets and investigating the different reaction behavior of mono- and dianionic guanidates. In this contribution, we describe our detailed studies into the synthesis of the first heterobimetallic lanthanide–lithium complexes containing the guanidinate dianion ligand and their reactivities with chlorosilanes, dichlorosilane, and benzoyl chloride. In these cases, the trisubstituted guanidinate dianion ligand undergoes a coupling reaction, cyclization, and transamination, to selectively transform into its tetrasubstituted monoanionic form, neutral heterocycles, and the acylamino ligand, respectively, which demonstrate the versatile reactivity of the dianionic guanidinate ligand owing to the accessibility of variable active sites. To our knowledge, the transformations of dianionic guanidinate ligands into organic heterocycles and acylamino groups have not been previously reported.

Results and Discussion

Synthesis and Characterization of Dianionic Guanidinate Lanthanide Complexes $\text{Cp}_2\text{Ln}[\mu-\eta^2:\eta^1-(\text{CyN})_2\text{CNPh}]\text{Li}(\text{THF})_3$. Reaction of Cp_3Ln with 1 equiv of $(\text{CyHN})_2\text{CNPh}$ in THF followed by treatment with 1 equiv of Li^nBu gave the expected dianionic guanidinate complexes $\text{Cp}_2\text{Ln}[\mu-\eta^2:\eta^1-(\text{CyN})_2\text{CNPh}]\text{Li}(\text{THF})_3$ ($\text{Ln} = \text{Yb}$ (**1a**), Er (**1b**), Y (**1c**), Dy (**1d**)) in moderate to good yields. Presumably, the formation of **1a–d** may result from the protonation reaction of Cp_3Ln with neutral guanidine and subsequent deprotonation, as shown in Scheme 1.

Compounds **1a–d** are sensitive to air and moisture and are soluble in THF and toluene and slightly soluble in *n*-hexane. Compounds **1a–d** were characterized by elemental analysis and spectroscopic methods. Their elemental analyses are in good agreement with the suggested molecular formulas. The $-\text{NCN}-$ characteristic stretching frequency of the dianionic guanidinate ligand was observed at ca. 1545 cm^{-1} ⁶ and was

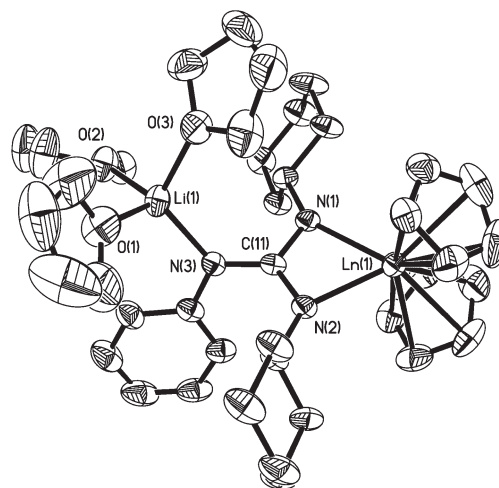


Figure 1. Thermal ellipsoid (30%) plot of $\text{Cp}_2\text{Ln}[(\text{CyN})_2\text{C}(\text{NPh})]\text{Li}(\text{THF})_3$ ($\text{Ln} = \text{Yb}$ (**1a**), Er (**1b**), Y (**1c**), Dy (**1d**)). Hydrogen atoms are omitted for clarity.

Table 1. Selected Bond Lengths and Angles for **1a**, **1b**, **1c**, and **1d**

	1a	1b	1c	1d
Bond Lengths (Å)				
Ln(1)–N(1)	2.247(7)	2.254(5)	2.278(4)	2.29(1)
Ln(1)–N(2)	2.267(7)	2.272(5)	2.282(4)	2.29(1)
N(1)–C(11)	1.369(10)	1.369(7)	1.349(7)	1.34(1)
N(2)–C(11)	1.347(11)	1.356(7)	1.340(6)	1.35(1)
N(3)–C(11)	1.373(11)	1.371(8)	1.375(7)	1.38(1)
N(3)–Li(1)	2.02(2)	2.03(1)	2.03(1)	2.03(2)
Li(1)–O(1)	1.99(2)	1.96(1)	1.98(1)	2.00(2)
Li(1)–O(2)	1.97(2)	1.97(1)	1.97(1)	2.00(2)
Li(1)–O(3)	1.99(2)	1.97(1)	1.96(1)	1.92(2)
Bond Angles (deg)				
N(1)–Ln(1)–N(2)	59.4(2)	59.5(2)	58.5(2)	58.4(2)
N(2)–C(11)–N(1)	110.9(8)	111.0(5)	111.9(5)	112.0(7)
N(2)–C(11)–N(3)	126.7(8)	126.2(5)	126.0(5)	125.9(7)
N(1)–C(11)–N(3)	122.1(8)	122.7(5)	122.0(5)	122.0(7)
C(11)–N(3)–Li(1)	125.6(7)	123.9(5)	123.1(4)	121.2(8)

slightly red-shifted as compared with those of the monoanionic guanidinate ligands.¹¹ Moreover, the medium bands at about 1075 and 890 cm^{-1} could be defined for coordinated THF molecules. The ^1H NMR spectrum of **1c** showed the cyclopentadienyl, cyclohexyl, phenyl, and THF resonances in the expected 2:2:1:3 ratio.

These heterobimetallic complexes were further confirmed by the X-ray single-crystal structural determination. The molecular structures are shown in Figure 1, and selected bond distances and angles for each are given in Table 1. Complexes **1a**, **1b**, **1c**, and **1d** are isostructural. Complex **1c** is

(9) Collin, J.; Daran, J. C.; Jacquet, O.; Schulz, E.; Trifonov, A. *Chem.—Eur. J.* **2005**, *11*, 3455.

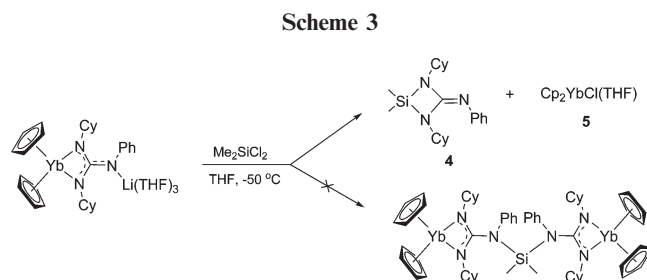
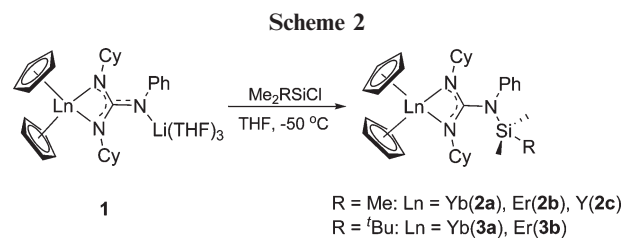
(10) (a) Pi, C. F.; Zhang, Z. X.; Pang, Z.; Zhang, J.; Luo, J.; Chen, Z. X.; Weng, L. H.; Zhou, X. G. *Organometallics* **2007**, *26*, 1934. (b) Pi, C. F.; Liu, R. T.; Zheng, P. Z.; Chen, Z. X.; Zhou, X. G. *Inorg. Chem.* **2007**, *46*, 5252. (c) Pi, C. F.; Zhu, Z. Y.; Weng, L. H.; Chen, Z. X.; Zhou, X. G. *Chem. Commun.* **2007**, 2190.

(11) Chang, C. C.; Hsiung, C. S.; Su, H. L.; Srinivas, B.; Chiang, M. Y.; Lee, G. H.; Wang, Y. *Organometallics* **1998**, *17*, 1595.

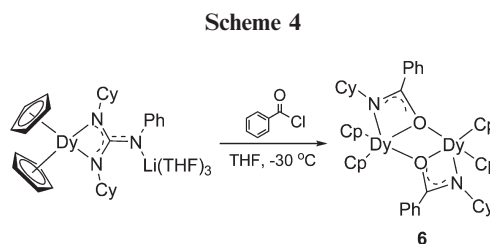
a heterodinuclear species possessing one bridging dianionic guanidinate ligand, in which two of the nitrogen atoms, N(1) and N(2), bond to the lanthanide center while the third N(3) coordinates the Li center. The coordination geometry of the Ln center can be described as a distorted tetrahedron. The individual Ln center is in geometries reminiscent of the previously reported monoanionic guanidinate lanthanide complexes that have cyclopentadienyl ligands as the ancillary ligands.¹² The ligand spans axial equatorial sites with a bite angle [N(1)–Y–N(2)] of 58.5(2)°. The central C atom of the dianionic guanidinate CN₃ core is planar. Furthermore, three N atoms exhibit very similar geometric parameters. In contrast to the observation that the dianionic guanidinate ligand has localized C–N single and double bonds in mononuclear complexes such as Pt[C(NPh)₃](COD)¹³ and Ta-(NMe₂)₃[(CyN)₂C(NCy)],^{7a,14} the C(11)–N(1), C(11)–N(2), and C(11)–N(3) distances of the dianionic guanidinate group in **1c** are approximately equivalent and significantly shorter than the C–N single-bond distances, indicating that the π electrons of the C=N double bond in the present structure are delocalized over the CN₃ unit.¹⁵ Consistent with this observation, the Y–N(1) and Y–N(2) distances, 2.278(4) and 2.282(4) Å, are between the values observed for the Y–N single-bond distance and the Y–N donor bond distance¹⁶ and are comparable to the corresponding values found in Cp₂Ln[(ⁱPrN)₂CNⁱPr₂] (Ln = Yb, Dy),^{12,17} when the difference in the metal ionic radii is considered.¹⁸ The cent–Ln–cent (cent = the center of cyclopentadienyl ring) plane relative to the LnNCN plane is approximately perpendicular. This disposition is likely the result of steric interactions between bulky isopropyl groups and two cyclopentadienyl ligands. The Li counterion is coordinated via three THF molecules and an N(3) atom.

The geometry and the stereochemistry of **1a**, **1b**, and **1d** are not particularly different from those observed in **1c**. In particular, the bonding mode of the dianionic guanidinate to metal ions is quite similar (Table 1).

Reactivity of Complexes 2 toward Chlorosilanes. Dianionic guanidinate complexes are rare, and only a few are found to lead to bridging structures.¹⁰ **1a–d** represent the first heterobimetallic lanthanide–lithium complexes containing the guanidinate dianion ligand. In order to obtain insight into the properties of bridged guanidinate metal complexes, we examine the reaction of Cp₂Ln[μ - η^2 : η^1 -(CyN)₂CNPh]Li(THF)₃ with electrophiles. Treatment of **1a–c** with 1 equiv of chlorotrimethylsilane gave the monoanionic guanidinate



complexes Cp₂Ln[(CyN)₂CN(Ph)SiMe₃] (Ln = Yb (**2a**), Er



(**2b**), Y (**2c**)) in moderate to good yields (Scheme 2). Furthermore, reaction of **1a** and **1b** with 1 equiv of ^tBuMe₂SiCl afforded the corresponding tetrasubstituted guanidinate complexes Cp₂Ln[(CyN)₂CN(Ph)SiMe₂^tBu] (Ln = Yb (**3a**), Er (**3b**)). These results indicate that the Li–N bond is preferentially attacked by the electrophiles rather than the Ln–N bond in the present system. The solid-state structures of **2** and **3** have been determined by X-ray analyses (Figures 2 and 3, Table 2).

As shown in Figure 2, complexes **2a–c** are isostructural, in which the newly formed silyl-substituted guanidinate anion acts as a chelating bidentate ligand to coordinate to the Cp₂Ln unit. For each of these compounds the C(11)–N(1) distance is comparable to the C(11)–N(2) length and shorter than the value of C(11)–N(3). These features are consistent with the negative charge of the ligand delocalized on the N(1) and N(2) atoms, which are bonded to Ln³⁺.

As shown in Figure 3, compounds **3a** and **3b** are also isostructural, and the lanthanide atom is coordinated by two η^5 -C₅H₅ groups and one chelating η^2 -(CyN)₂CN(Ph)-SiMe₂^tBu ligand, and its coordination number is 8. The geometry and the stereochemistry of **3** are not particularly different from those observed in **2**, and the bonding mode of the guanidinate to the metal ion is quite similar (Table 2). The C(11)–N(3)–Si(1) angle is slightly larger than the corresponding value in **2**, due to the greater hindrance of the SiMe₂^tBu compared with SiMe₃ substituent.

Reactivity of Complexes 1 toward Dichlorosilanes. Controlling the metal coordination environment and reactivity through modification of supporting ligation is an important strategy in organometallic chemistry. Considerable interest has focused on the tailoring of two independent monoanion ligands to a defining and constraining linked dianion ligand

(12) Zhang, J.; Cai, R. F.; Weng, L. H.; Zhou, X. G. *Organometallics* **2004**, *23*, 3303.

(13) Dinger, M. B.; Henderson, W.; Nicholson, B. K. *J. Organomet. Chem.* **1998**, *556*, 75.

(14) Tin, M. K. T.; Yap, G. P. A.; Richeson, D. S. *Inorg. Chem.* **1998**, *37*, 6728.

(15) (a) Thirupathi, N.; Yap, G. P. A.; Richeson, D. S. *Chem. Commun.* **1999**, 2483. (b) Rodriguez, G.; Sperry, C. K.; Bazan, G. C. *J. Mol. Catal. A: Chem.* **1998**, *128*, 5. (c) Foley, S. R.; Yap, G. P. A.; Richeson, D. S. *Inorg. Chem.* **2002**, *41*, 4149.

(16) (a) Evans, W. J.; Drummond, D. K.; Chamberlain, L. R.; Doedens, R. J.; Bott, S. G.; Zhang, H. M.; Atwood, J. L. *J. Am. Chem. Soc.* **1988**, *110*, 4983. (b) Zhou, X. G.; Huang, Z. E.; Cai, R. F.; Zhang, L. X.; Hou, X. F.; Feng, X. J.; Huang, X. Y. *J. Organomet. Chem.* **1998**, *563*, 101. (c) Zhou, X. G.; Huang, Z. E.; Cai, R. F.; Zhang, L. B.; Zhang, L. X.; Huang, X. Y. *Organometallics* **1999**, *18*, 4128. (d) Wang, Y. R.; Shen, Q.; Xue, F.; Yu, K. B. *J. Organomet. Chem.* **2000**, *598*, 359.

(17) Zhang, J.; Cai, R. F.; Weng, L. H.; Zhou, X. G. *J. Organomet. Chem.* **2003**, *672*, 94.

(18) Shannon, R. D. *Acta Crystallogr., Sect. A: Found. Crystallogr.* **1976**, *32*, 751.

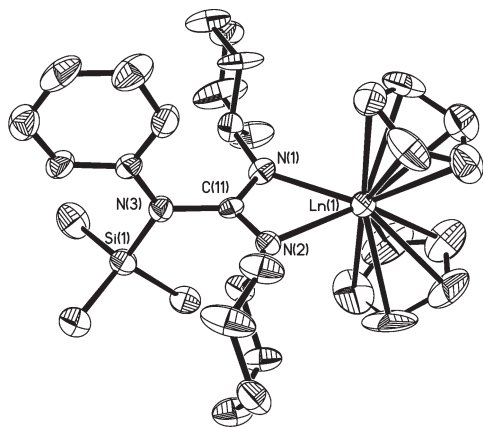


Figure 2. Thermal ellipsoid (30%) plot of $\text{Cp}_2\text{Ln}[(\text{CyN})_2\text{CN}-(\text{Ph})\text{SiMe}_3]$ ($\text{Ln} = \text{Yb}$ (**2a**), Er (**2b**), Y (**2c**)). Hydrogen atoms are omitted for clarity.

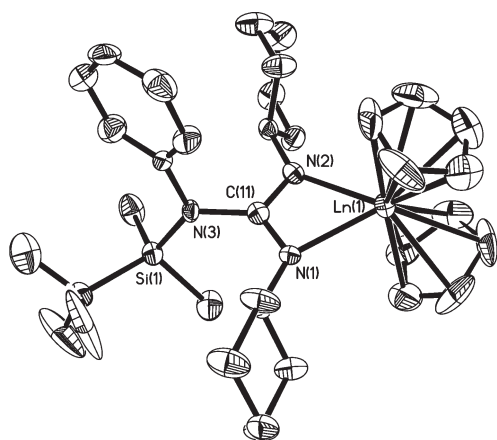


Figure 3. Thermal ellipsoid (30%) plot of $\text{Cp}_2\text{Ln}[(\text{CyN})_2\text{CN}-(\text{Ph})\text{SiMe}_2^t\text{Bu}]$ ($\text{Ln} = \text{Yb}$ (**3a**), Er (**3b**)). Hydrogen atoms are omitted for clarity.

Table 2. Selected Bond Lengths and Angles for **2a**, **2b**, **2c**, **3a**, and **3b**

	2a	2b	2c	3a	3b
Bond Lengths (Å)					
Ln(1)–N(1)	2.296(8)	2.299(4)	2.334(6)	2.299(5)	2.307(4)
Ln(1)–N(2)	2.312(7)	2.316(4)	2.343(6)	2.280(5)	2.299(4)
N(1)–C(11)	1.340(10)	1.322(6)	1.342(8)	1.324(7)	1.336(5)
N(2)–C(11)	1.298(11)	1.329(6)	1.315(8)	1.337(7)	1.337(5)
N(3)–C(11)	1.431(11)	1.455(6)	1.453(9)	1.456(7)	1.445(5)
Si(1)–N(3)	1.765(7)	1.756(4)	1.737(6)	1.757(5)	1.770(3)
Bond Angles (deg)					
N(1)–Ln(1)–N(2)	58.4(3)	57.89(15)	57.5(2)	58.6(2)	58.27(12)
N(2)–C(11)–N(1)	116.9(8)	114.8(5)	115.8(7)	114.9(6)	114.1(4)
N(2)–C(11)–N(3)	122.3(8)	122.0(5)	123.2(8)	120.5(6)	121.5(4)
N(1)–C(11)–N(3)	120.8(8)	123.2(5)	121.0(7)	124.6(6)	124.4(4)
C(11)–N(3)–Si(1)	120.3(5)	120.6(3)	119.0(5)	122.8(4)	122.1(3)

for further perfecting the versatility of these ligands. Such concepts have been elegantly applied to *ansa*-metallocene complexes¹⁹ and other anionic functionalities including

(19) (a) Qian, C. T.; Nie, W. L.; Sun, J. *J. Organomet. Chem.* **2001**, *626*, 171. (b) Qian, C. T.; Nie, W. L.; Chen, Y. F.; Sun, J. *J. Organomet. Chem.* **2002**, *645*, 82. (c) Nie, W. L.; Qian, C. T.; Chen, Y. F.; Jie, S. *J. Organomet. Chem.* **2002**, *647*, 114.

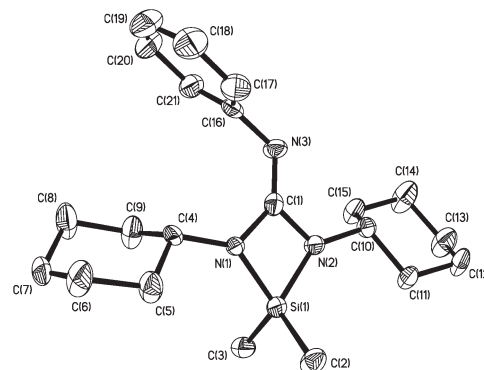


Figure 4. Thermal ellipsoid (30%) plot of $\text{Me}_2\text{Si}(\text{CyN})_2\text{C}=\text{NPh}$ (**4**). Hydrogen atoms are omitted for clarity. Selected bond lengths (Å) and angles (deg): Si(1)–N(2) 1.721(3), Si(1)–N(1) 1.749(3), N(1)–C(1) 1.420(5), N(2)–C(1) 1.410(4), N(3)–C(1) 1.257(4), N(2)–Si(1)–N(1) 76.3(2), N(2)–C(1)–N(1) 98.4(4), C(1)–N(3)–C(16) 121.3(4).

aryloxides,²⁰ amidinates,²¹ amides, and imides.²² However, there are few reports employing linked diguanidinate dianion analogues.^{10b} Encouraged by the above result, we were interested in establishing whether two of these dianionic guanidinate ligands could be linked together by reaction with dichlorosilane. In contrast to Me_3SiCl and $^t\text{BuMe}_2\text{SiCl}$, reaction of **1a** with 1 equiv of Me_2SiCl_2 in THF yielded $\text{Cp}_2\text{YbCl}(\text{THF})$ (**5**) as the main lanthanide-containing product without the formation of the expected linked diguanidinate complex, even with only 0.5 equiv or less of Me_2SiCl_2 used. The results indicate that Me_2SiCl_2 is preferably coupled to one guanidinate dianion ligand through the two nitrogen atoms of the NCy groups rather than the NPh to form the silicon-containing heterocycle **4**. These features are consistent with negative charges of the guanidinate dianion ligand of **1** delocalized on the three N atoms and, thus, demonstrate that the active site of the ligand is tunable. Complex **5** was characterized by X-ray diffraction.²³ Single crystals of the resulting organic heterocycle $\text{Me}_2\text{Si}(\text{CyN})_2\text{C}(\text{NPh})$ (**4**) (Figure 4) were also obtained by extraction of the reaction mixture with toluene.

Figure 4 confirms clearly that the Me_2SiCl_2 is coupled to the two nitrogen atoms of the NCy groups rather than the anticipated nitrogen of the NPh group, and the selectivity is different from that observed in reaction of **1a** with Me_3SiCl . The short N(3)–C(1) distance (1.257(4) Å) and the planar geometry of the C(1) (sum of angles 360°) are consistent with a localized double bond between these two atoms.

(20) Evans, W. J.; Greci, M. A.; Ziller, J. W. *J. Chem. Soc., Dalton Trans.* **1997**, 3035.

(21) (a) McNevin, M. J.; Hagadorn, J. R. *Inorg. Chem.* **2004**, *43*, 8547. (b) Hagadorn, J. R.; McNevin, M. J.; Wiedenfeld, G.; Shoemaker, R. *Organometallics* **2003**, *22*, 4818. (c) Hagadorn, J. R.; McNevin, M. J. *Organometallics* **2003**, *22*, 609. (d) Grundy, J.; Coles, M. P.; Hitchcock, P. B. *J. Organomet. Chem.* **2002**, *662*, 178. (e) Clare, B.; Sarker, N.; Shoemaker, R.; Hagadorn, J. R. *Inorg. Chem.* **2004**, *43*, 1159. (f) Chen, C. T.; Huang, C. A.; Tzeng, Y. R.; Huang, B. H. *Dalton Trans.* **2003**, 2585.

(22) (a) Zhao, B.; Li, H. H.; Shen, Q.; Zhang, Y.; Yao, Y. M.; Lu, C. R. *Organometallics* **2006**, *25*, 1824. (b) Hogarth, G.; Humphrey, D. G.; Kaltsoyannis, N.; Kim, W. S.; Lee, M. Y.; Norman, T.; Redmond, S. P. *J. Chem. Soc., Dalton Trans.* **1999**, 2705. (c) Dorado, I.; Garces, A.; Lopez-Mardomingo, C.; Fajardo, M.; Rodriguez, A.; Antinolo, A.; Otero, A. *J. Chem. Soc., Dalton Trans.* **2000**, 2375. (d) Antinolo, A.; Dorado, I.; Fajardo, M.; Garces, A.; Lopez-Solera, I.; Lopez-Mardomingo, C.; Kubicki, M. M.; Otero, A.; Prashar, S. *Eur. J. Inorg. Chem.* **2004**, 1299.

(23) Stellfeldt, D.; Meyer, G.; Deacon, G. B. *Z. Anorg. Allg. Chem.* **2001**, *627*, 1659.

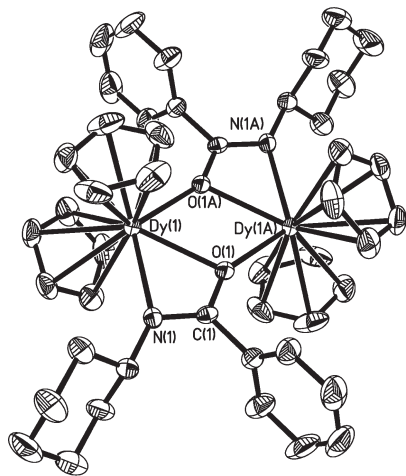


Figure 5. Thermal ellipsoid (30%) plot of $[\text{Cp}_2\text{Dy}(\text{OC}(\text{Ph})\text{NCy})_2]$ (**6**). Hydrogen atoms are omitted for clarity. Selected bond lengths (Å) and angles (deg): Dy1–O1A 2.327(3), Dy1–O1 2.422(3), Dy1–N1 2.490(4), N1–C1 1.268(5), O1–C1 1.312(5), O1A–Dy1–O1 67.6(1), O1A–Dy1–N1 120.3(1), O1–Dy1–N1 53.2(1), C1–N1–Dy1 94.0(3), C1–O1–Dy1A 150.9(3), C1–O1–Dy1 95.9(2), Dy1A–O1–Dy1 112.4(1), N1–C1–O1 116.9(4), N1–C1–Dy1 59.9(2), O1–C1–Dy1 57.0(2).

The distances of the N(1)–C(1) and N(2)–C(1) bonds are in the typical C–N single-bond range. The average Si–N distance of 1.735(3) Å is comparable to the values found in $[\{\text{Ln}(\eta^2\text{-C}_3\text{N}_2\text{HMe}_2\text{-}3,5)(\mu\text{-}\eta^1\text{-}\eta^2\text{-OSiMe}_2\text{C}_3\text{N}_2\text{HMe}_2\text{-}3,5)(\eta\text{-C}_5\text{H}_4\text{Me})\}_2]$ (Ln = Yb, Dy), 1.792(6) Å,²⁴ but is significantly shorter than the Si–N donor bond distances.²⁵

Reactivity of Complexes 1 toward Benzoyl Chloride. To further reveal the reactivity of **1**, we attempted to introduce an acyl substituent on the nitrogen atom of the guanidinate dianion ligands with benzoyl chloride. We anticipated that this would allow a straightforward avenue for future modifications. However, treatment of **1d** with PhCOCl led to the disruptive acylation of the dianionic guanidinate ligand, to afford the corresponding acylamino complex $[\text{Cp}_2\text{Dy}(\text{OC}(\text{Ph})\text{NCy})_2]$ (**6**), indicating that the dianionic guanidinate ligand underwent a tandem acylation/elimination of cyclohexylphenylcarbodiimide moiety. Although the details of the reaction mechanism are not yet clear, the reaction system described here is the first example in which the coordinated guanidinate dianion is converted into acylamido.

Complex **6** was characterized by elemental analysis and spectroscopic properties, which were in good agreement with the proposed structures. In the IR spectral data, the O–C–N stretching vibration of the coordinated acylamino groups is observed at 1606 cm^{-1} .²⁶ Direct confirmation of the structural features of **6** was obtained through a single-crystal X-ray study. The results are summarized in Figure 5. Examination of Figure 5 shows that the pseudo-trigonal-bipyramidal coordination geometry of the Dy center is defined by a bidentate acylamino anion and two Cp ligands, with one coordination site occupied by an oxygen atom from another acylamino ligand. The acylamino ligand is bonded to Dy

through one nitrogen atom and one bridging oxygen to yield a planar four-membered cycle of sp^2 -hybridized N and C centers with a bite angle of $117.0(8)^\circ$. The bond distances within the OCN moiety (N(1)–C(1) 1.26 Å, O(1)–C(1) 1.31 Å) are in agreement with a delocalized π interaction.

Conclusions

In summary, we have synthesized the first heterobimetallic lanthanide–lithium complexes containing the guanidinate dianion ligand. Furthermore, some novel reactivity features of dianionic guanidinate ligands, such as the coupled cyclization with dichlorosilane and the acylation/decarbodiimination with benzoyl chloride, have also been established. These results have shown that deprotonation of monoanionic guanidinate ligands is a convenient and applicable methodology for synthesis of guanidinate dianion complexes of rare earth elements. On the basis of the reactions with Me_3SiCl , Me_2SiCl_2 , and PhCOCl it would appear that the active site of the dianionic guanidinate ligand is tunable due to the delocalization of the two negative charges on the three N atoms. The dianionic cooperative effect not only tends to increase the coordination and reactivity availability in the guanidinate ligand but delicately induces some unusual tandem reactions.

Experimental Section

General Remarks. All operations involving air- and moisture-sensitive compounds were carried out under an inert atmosphere of purified nitrogen gas using standard Schlenk techniques. The solvents THF, toluene, and *n*-hexane were refluxed and distilled over sodium benzophenone ketyl under nitrogen gas prior to use. Elemental analyses for C, H, and N were carried out on a Vario EL III elemental analyzer (Analysensysteme GmbH, Germany). Infrared spectra were recorded on a Nicolet Avatar-360 FT-IR spectrometer with samples prepared in Nujol mulls. ¹H NMR and ¹³C NMR spectra were recorded on a JEOL ECA400 NMR spectrometer (FT, 400 MHz for ¹H; 100 MHz for ¹³C). The chemical shifts are reported in ppm referenced to tetramethylsilane. The starting materials Cp_3Ln ²⁷ and neutral guanidines were prepared according to the literature methods.²⁸ All amines and carbodiimides used were purchased from commercial sources and were used without further purification.

Preparation of $\text{Cp}_2\text{Yb}[(\text{CyN})_2\text{C}(\text{NPh})]\text{Li}(\text{THF})_3$ (1a**).** A 1:1 mixture of Cp_3Yb (0.482 g, 1.31 mmol) and *N,N'*-dicyclohexyl-*N''*-phenylguanidine (0.392 g, 1.31 mmol) was dissolved in 30 mL of THF and was stirred at 50 °C for 2 h. After the volatile materials were removed under vacuum, the residue was dissolved in 30 mL of THF. To the above solution was added dropwise *n*-butyllithium (2.5 M in hexane, 0.52 mL, 1.31 mmol) at –78 °C. After stirring at low temperature for 30 min, the reaction mixture was slowly warmed to room temperature and stirred for another 12 h. Then, the solution was concentrated to ca. 2 mL and was stored at –15 °C. **1a** was obtained as dark red crystals. Yield: 0.87 g (81%). Anal. Calcd for $\text{C}_{41}\text{H}_{61}\text{LiN}_3\text{O}_3\text{Yb}$: C, 59.77; H, 7.46; N, 5.10. Found: C, 59.67; H, 7.49; N, 5.08. IR (Nujol): 3087 w, 3062 w, 3042 w, 1594 m, 1534 m, 1460 s, 1378 s, 1308 m, 1215 m, 1176 m, 1073 m, 1049 m, 1011 m, 890 m, 766 m, 693 m, cm^{-1} .

Preparation of $\text{Cp}_2\text{Er}[(\text{CyN})_2\text{C}(\text{NPh})]\text{Li}(\text{THF})_3$ (1b**).** Following the method described for **1a**, using Cp_3Er (0.359 g, 0.99 mmol), *N,N'*-dicyclohexyl-*N''*-phenylguanidine (0.296 g,

(24) (a) Zhou, X. G.; Ma, H. Z.; Huang, X. Y.; You, X. Z. *J. Chem. Soc., Chem. Commun.* **1995**, 2483. (b) Zhou, X. G.; Ma, W. W.; Huang, Z. E.; Cai, R. F.; You, X. Z.; Huang, X. Y. *J. Organomet. Chem.* **1997**, 545, 309.

(25) Maaranen, J.; Andell, O. S.; Vanne, T.; Mutikainen, I. *J. Organomet. Chem.* **2006**, 691, 240.

(26) Zhou, X. G.; Zhang, L. B.; Zhu, M.; Cai, R. F.; Weng, L. H.; Huang, Z. X.; Wu, Q. *J. Organometallics* **2001**, 20, 5700.

(27) Birmingham, J. M.; Wilkinson, G. *J. Am. Chem. Soc.* **1956**, 78, 42.

(28) Li, Q. H.; Wang, S. W.; Zhou, S. L.; Yang, G. S.; Zhu, X. C.; Liu, Y. Y. *J. Org. Chem.* **2007**, 72, 6763.

0.99 mmol), and *n*-butyllithium (2.5 M in hexane, 0.40 mL, 1.00 mmol) afforded **1b** as pink crystals. Yield: 0.70 g (87%). Anal. Calcd for $C_{41}H_{61}ErLiN_3O_3$: C, 60.19; H, 7.52; N, 5.14. Found: C, 60.15; H, 7.50; N, 5.13. IR (Nujol): 3088 w, 3063 w, 3042 w, 1593 m, 1547 m, 1460 s, 1378 s, 1308 m, 1213 m, 1176 m, 1072 m, 1049 m, 1011 m, 889 m, 765 m, 693 m, cm^{-1} .

Preparation of $Cp_2Y[(CyN)_2C(NPh)]Li(THF)_3$ (1c**).** Following the method described for **1a**, using Cp_3Y (0.617 g, 2.17 mmol), *N,N'*-dicyclohexyl-*N''*-phenylguanidine (0.649 g, 2.17 mmol), and *n*-butyllithium (2.5 M in hexane, 0.87 mL, 2.17 mmol) afforded **1c** as colorless crystals. Yield: 1.28 g (79%). Anal. Calcd for $C_{41}H_{61}LiN_3O_3Y$: C, 66.56; H, 8.31; N, 5.68. Found: C, 66.51; H, 8.34; N, 5.65. 1H NMR (C_6D_6 , 7.16): δ 7.97 (m, 2H, C_6H_5), 7.84 (m, 1H, C_6H_5), 7.40 (m, 2H, C_6H_5), 7.17 (s, 5H, C_5H_5), 7.15 (s, 5H, C_5H_5), 4.20 (m, 12H, THF), 3.83 (m, 2H, C_6H_{11}), 2.76 (m, 8H, C_6H_{11}), 2.40 (m, 4H, C_6H_{11}), 2.06 (m, 12H, THF), 1.87 (m, 8H, C_6H_{11}). ^{13}C NMR (THF- d_8): δ 171.4, 156.8, 127.8, 123.7, 114.4, 109.7, 67.2, 53.5, 37.3, 26.3, 26.1, 25.4. IR (Nujol): 3087 w, 3062 w, 3042 w, 1593 m, 1546 m, 1460 s, 1377 s, 1307 m, 1211 m, 1176 m, 1073 m, 1049 m, 1011 m, 888 m, 764 m, 693 m, cm^{-1} .

Preparation of $Cp_2Dy[(CyN)_2C(NPh)]Li \cdot THF_3$ (1d**).** Following the method described for **1a**, using Cp_3Dy (0.479 g, 1.34 mmol), *N,N'*-dicyclohexyl-*N''*-phenylguanidine (0.400 g, 1.34 mmol), and *n*-butyllithium (2.5 M in hexane, 0.54 mL, 1.35 mmol) afforded colorless crystals of **1d**. Yield: 0.94 g (86%). Anal. Calcd for $C_{41}H_{61}DyLiN_3O_3$: C, 60.54; H, 7.56; N, 5.17. Found: C, 60.48; H, 7.54; N, 5.18. IR (Nujol): 3087 w, 3062 w, 3042 w, 1593 m, 1546 m, 1460 s, 1377 s, 1307 m, 1211 m, 1176 m, 1073 m, 1047 m, 1010 m, 887 m, 761 m, 693 m, cm^{-1} .

Preparation of $Cp_2Yb[(CyN)_2C(NPh)SiMe_3]$ (2a**).** To a THF (30 mL) solution of **1a** (0.88 mmol) held at $-50^\circ C$ was added dropwise chlorotrimethylsilane (0.11 mL, 0.88 mmol). The reaction mixture was slowly warmed to room temperature and stirred for 24 h. The solvent was evaporated under vacuum. The oily residue was extracted with toluene (30 mL), and the precipitate was removed by centrifugation. The solution was concentrated by reduced pressure to about 1 mL, and a white solid precipitated. The precipitate was resolved by addition of several drops of THF, and red crystals of **2a** were obtained upon cooling at $-15^\circ C$. Yield: 0.50 g (84%). Anal. Calcd for $C_{32}H_{46}N_3SiYb$: C, 57.04; H, 6.88; N, 6.24. Found: C, 57.08; H, 6.86; N, 6.23. IR (Nujol): 3087 m, 3074 m, 2840 s, 1642 m, 1599 s, 1578 s, 1551 m, 1455 s, 1378 s, 1360 s, 1308 m, 1255 s, 1197 s, 1141 s, 1076 m, 1046 m, 1034 m, 1009 m, 981 m, 928 m, 900 m, 889 m, 838 m, 767 m, 695 m, 674 m, 644 m, 616 m, cm^{-1} .

Preparation of $Cp_2Er[(CyN)_2C(NPh)SiMe_3]$ (2b**).** Following the method described for **2a**, reaction of **1b** (0.95 mmol) with chlorotrimethylsilane (0.12 mL, 0.95 mmol) afforded **2b** as pink crystals. Yield: 0.52 g (81%). Anal. Calcd for $C_{32}H_{46}ErN_3Si$: C, 57.53; H, 6.94; N, 6.29. Found: C, 57.51; H, 6.96; N, 6.28. IR (Nujol): 3090 m, 3076 m, 2842 s, 1644 m, 1599 m, 1578 m, 1557 m, 1444 s, 1380 s, 1360 s, 1307 m, 1254 s, 1189 s, 1141 s, 1075 m, 1046 m, 1034 m, 1008 m, 979 m, 928 m, 900 m, 889 m, 840 m, 727 m, 694 m, 674 m, 644 m, 616 m, cm^{-1} .

Preparation of $Cp_2Y[(CyN)_2C(NPh)SiMe_3]$ (2c**).** Following the method described for **2a**, reaction of **1c** (1.34 mmol) with chlorotrimethylsilane (0.17 mL, 1.34 mmol) afforded **2c** as pale yellow crystals. Yield: 0.53 g (67%). Anal. Calcd for $C_{32}H_{46}N_3SiY$: C, 65.17; H, 7.86; N, 7.13. Found: C, 65.19; H, 7.83; N, 7.11. 1H NMR (C_6D_6 , 7.16): δ 7.14 (m, 2H, C_6H_5), 7.02 (m, 1H, C_6H_5), 6.74 (m, 2H, C_6H_5), 6.39 (s, 5H, C_5H_5), 6.30 (s, 5H, C_5H_5), 3.06 (m, 2H, C_6H_{11}), 1.64 (m, 8H, C_6H_{11}), 1.45 (m, 4H, C_6H_{11}), 0.98 (m, 8H, C_6H_{11}), 0.39 (s, 9H, CH_3). ^{13}C NMR (THF- d_8): δ 158.1, 145.7, 128.6, 118.3, 115.5, 110.7, 55.2, 37.4, 37.2, 25.8, 25.7, 25.6, 0.3. IR (Nujol): 3090 m, 3076 m, 3022 m,

2839 s, 1642 m, 1599 s, 1578 s, 1546 m, 1461 s, 1379 s, 1355 s, 1307 m, 1253 s, 1195 s, 1141 s, 1089 m, 1075 m, 1046 m, 1034 m, 1009 m, 980 m, 929 m, 900 m, 888 m, 840 m, 767 m, 733 m, 696 m, 674 m, 644 m, 616 m, cm^{-1} .

Preparation of $Cp_2Yb[(CyN)_2C(NPh)SiMe_2^tBu]$ (3a**).** Following the method described for **2a**, reaction of **1a** (1.15 mmol) with *tert*-butyldimethylchlorosilane (0.91 mL, 1.15 mmol) gave **3a** as brown-yellow crystals. Yield: 0.72 g (88%). Anal. Calcd for $C_{35}H_{52}N_3SiYb$: C, 58.72; H, 7.32; N, 5.87. Found: C, 58.69; H, 7.32; N, 5.89. IR (Nujol): 3095 w, 2854 s, 1638 m, 1596 m, 1576 m, 1461 s, 1378 s, 1343 m, 1306 m, 1257 m, 1227 m, 1195 m, 1139 s, 1073 m, 1048 w, 1031 w, 1010 m, 978 m, 937 w, 919 m, 890 m, 836 m, 811 m, 802 m, 770 s, 733 m, 695 m, 674 m, 611 m, cm^{-1} .

Preparation of $Cp_2Er[(CyN)_2C(NPh)SiMe_2^tBu]$ (3b**).** Following the method described for **2a**, reaction of **1b** (1.34 mmol) with *tert*-butyldimethylchlorosilane (1.06 mL, 1.34 mmol) afforded **3b** as pink crystals. Yield: 0.89 g (94%). Anal. Calcd for $C_{35}H_{52}ErN_3Si$: C, 59.20; H, 7.38; N, 5.92. Found: C, 59.27; H, 7.35; N, 5.91. IR (Nujol): 3093 w, 3074 w, 3091 w, 2859 s, 1648 w, 1597 s, 1577 m, 1465 s, 1378 s, 1325 m, 1306 m, 1265 m, 1216 s, 1190 m, 1141 m, 1088 m, 1056 s, 1033 m, 1011 s, 970 m, 942 m, 919 m, 878 m, 834 m, 819 m, 807 m, 768 s, 725 m, 699 m, 675 m, 614 m, cm^{-1} .

Preparation of $Me_2Si(CyN)_2C=NPh$ (4**).** To a THF (30 mL) solution of **1a** (1.10 mmol) held at $-50^\circ C$ was added dropwise dimethyldichlorosilane (0.065 mL, 0.55 mmol). After stirring for 24 h, the solvent was evaporated under vacuum, and the oily residue was extracted with toluene (30 mL). The clear solution was concentrated by reduced pressure to ca. 2 mL. The precipitate was redissolved with several drops of THF. The resulting solution was stored at $-15^\circ C$. **4** was obtained as colorless crystals. Yield: 0.17 g (86%). Anal. Calcd for $C_{21}H_{33}N_3Si$: C, 70.93; H, 9.35; N, 11.82. Found: C, 70.87; H, 9.32; N, 11.85. 1H NMR (C_6D_6): δ 7.24 (m, 2H, C_6H_5), 7.20 (m, 1H, C_6H_5), 6.92 (m, 2H, C_6H_5), 3.86 (m, 2H, C_6H_{11}), 1.49 (m, 8H, C_6H_{11}), 1.00 (m, 4H, C_6H_{11}), 0.87 (m, 8H, C_6H_{11}), 0.28 (s, 6H, CH_3). ^{13}C NMR ($CDCl_3$): δ 129.1, 128.2, 123.0, 121.9, 120.9, 50.7, 34.6, 25.8, 25.3, 2.0. IR (Nujol): 3055 w, 2856 s, 1638 m, 1588 m, 1463 s, 1376 s, 1347 m, 1304 m, 1254 m, 1147 m, 982 m, 764 m, 697 m, cm^{-1} .

Preparation of $[Cp_2Dy(PhCONCy)]_2$ (6**).** To a toluene (30 mL) solution of **1d** (1.27 mmol) held at $-30^\circ C$ was added dropwise benzoyl chloride (0.147 mL, 1.27 mmol), and the reaction solution was slowly warmed to room temperature and stirred for another 24 h. The precipitate was removed by centrifugation. The clear solution was concentrated by reduced pressure to about 2 mL. Cooling the solution at $-15^\circ C$ gave **6** as orange-red crystals. Yield: 0.64 g (51%). Anal. Calcd for $C_{46}H_{52}Dy_2N_2O_2$: C, 55.81; H, 5.29; N, 2.83. Found: C, 55.78; H, 5.30; N, 2.82. IR (Nujol): 2955 s, 2924 s, 2853 s, 1606 m, 1573 s, 1460 s, 1377 s, 1342 s, 1087 m, 1010 m, 769 m, cm^{-1} .

Crystallographic parameters for compounds **1a–d**, **2a–c**, **3a**, **3b**, **4**, and **6** along with details of the data collection and refinement are included in the Supporting Information.

Acknowledgment. We thank the National Natural Science Foundation of China, 973 program (2009CB825300), Shanghai Science and Technology Committee, the Research Fund for the Doctoral Program of Higher Education of China, and Shanghai Leading Academic Discipline Project (B108) for financial support.

Supporting Information Available: Tables of atomic coordinates and thermal parameters are available free of charge via the Internet at <http://pubs.acs.org>.